Macromolecules
ARTICLE

Macromolecules **2010**, *43*, 9511–9521 **9511**
DOI: 10.1021/ma1017549

Thermally Induced Swellability and Acid-Liable Dynamic Properties of Microgels of Copolymers Based on PEGMA and Aldehyde-Functionalized Monomer

Chaowei Cao, Ke Yang, Fen Wu, Xiangqian Wei, Lican Lu, and Yuanli Cai*

Key Laboratory of Environmentally Friendly Chemistry and Applications of Ministry of Education, Key Laboratory of Advanced Functional Polymeric Materials of College of Hunan Province, Key Laboratory of Polymeric Materials & Application Technology of Hunan Province, College of Chemistry, Xiangtan University, Xiangtan, Hunan 411105, China

Received August 2, 2010; Revised Manuscript Received October 5, 2010

ABSTRACT: This paper describes a new class of smart microgels that possess entirely reversible thermally induced swellability and acid-liable dynamic properties in aqueous solution. To this end, 3-(4-formylphenoxy)-2-hydroxypropyl methacrylate (FPHPMA) was synthesized. RAFT polymerization of FPHPMA, RAFT random copolymerization of FPHPMA and poly(ethylene glycol) methacrylate (PEGMA), and chain extension RAFT polymerization of PEGMA using P(FPHPMA-*ran*-PEGMA) as a macromolecular chain transfer agent proceeded under visible light radiation at 25 °C. The results indicated the well-controlled polymerization of FPHPMA, comparable reactivity of FPHPMA and PEGMA, and living character of these polymerizations under such mild conditions. Thus, a range of well-defined copolymers of FPHPMA and PEGMA with different chain length, composition, or sequence were synthesized. The aldehyde groups of copolymers were stable against air oxidation in aqueous solution at 80 °C. These copolymers well dissolved in water at low solution temperature and exhibited a cloud point (CP) and a critical solution temperature for the formation of compressed aggregates (T_c) upon heating. The thermally induced phase transition of random copolymers was slightly influenced by chain length but significantly depended on the composition or concentration. Moreover, the sequence of copolymers exerted essential control over this thermally induced phase transition. Contrary to the previously reported PEGMA-based copolymers, these copolymers exhibited significant hysteresis in cooling process similar to what observed in poly(*N*-isopropylacrylamide) (PNIPAM). However, its isotopic solvent effect was contrary to what was observed in PNIPAM. In these thermally induced aggregates, the aldehyde groups could react with hexamethylenediamine or adipoyl hydrazide, leading to the formation of microgels. These microgels exhibited entirely reversible thermally induced swellability. This swellability could be finely tuned by adjusting the solution pH.

Introduction

The polymers that contain poly(ethylene glycol) (PEG) have been extensively utilized in the biorelated fields because of their fascinating bioavailability, biocompatibility, and immunogenicity.[1,2] Recent studies revealed that poly(meth)acrylates containing short PEG side chains exhibit thermally induced phase transition.[3−15] Lutz and co-workers[12−15] demonstrated that their thermoresponsive behavior could be precisely adjusted by varying the comonomer composition based on PEG monomers of different chain lengths. Recently, Endo and co-workers[16] described the controlled release of aldehyde from poly(ethylene glycol) methacrylate (PEGMA)-based amphiphilic copolymer having acid-labile acetal pendent groups via thermoresponsive aggregation or dissociation of copolymer micelles. Most recently, Li and co-workers[17] reported that the polyacrylates with pendent PEG chains and cyclic ortho ester groups exhibited thermally induced liquid−liquid phase transition and acid liability. Liu and co-workers described the thermally induced swellability of cross-linked micelles of a copolymer that contains PEG blocks[18] or pH-tunable swellability of cross-linked micelles of a copolymer that contains PEGMA blocks and α-aldehyde chain ends.[19]

*Corresponding author: Ph +86-731-58298876; Fax +86-731-58292251; e-mail ylcai98@xtu.edu.cn.

Reactive functional groups, along the polymer backbone or at the chain ends, have been extensively utilized to conjugate compounds.[20] Particularly, the aldehyde groups may react rapidly with primary amine or hydrazine under mild conditions. In this respect, aldehyde groups have been shown to be versatile and convenient to covalently attach proteins,[21] enzymes,[22] or hyaluronic acid for nonradioactive DNA probes.[23] Kataoka and co-workers[24−27] synthesized PEG-based block copolymers that contain aldehyde groups at the PEG chain ends via protecting chemistry and anionic polymerization; their micellization behavior was extensively studied. However, to date, the synthesis of well-defined polymers from aldehyde-functionalized monomers has proven to be challenging.

The reversible addition−fragmentation chain transfer radical polymerization or RAFT polymerization[28] is a powerful tool for the synthesis of well-defined water-soluble or stimuli-responsive polymers,[29−33] including aldehyde-functionalized polymers.[34−36] A commonly used approach was the postconversion of protecting groups to aldehyde groups.[24−27,37−39] Recently, Wooley and co-workers[40] reported the first example of block copolymer bearing multiple aldehydes with predictable molecular weights and low polydispersities by direct RAFT polymerization. These copolymers were utilized for the fabrication of vesicles bearing benzaldehyde groups within vesicular walls.[41] Lu and co-workers

Published on Web 10/19/2010

Scheme 1. Schematic Illustration for the Synthesis of 3-(4-Formylphenoxy)-2-hydroxypropyl Methacrylate (FPHPMA) Monomer and Its Visible Light Activating RAFT Polymerization at 25 °C

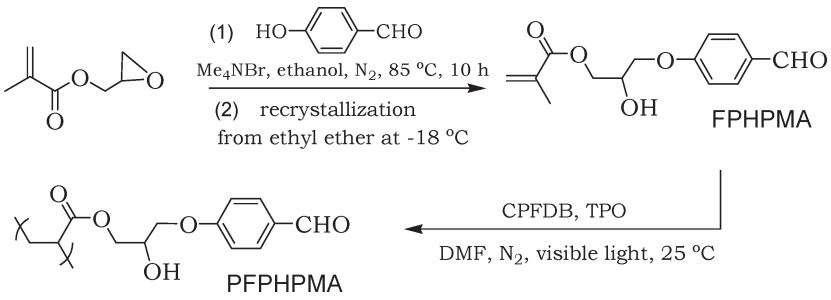

reported the polymerization of monomer containing benzaldehyde and ferrocene groups[42] or aldehyde-functionalized glycomonomer[43] in a time-consuming RAFT process.

In recent years, our group exploited a highly effecient and well-controlled visible light activating ambient temperature RAFT polymerization.[44−47] Under such mild conditions, poly(ethylene glycol) acrylate (PEGA) monomer polymerized in a ultrafast and well-controlled fashion, e.g., shortly in several minutes to high monomer conversions.[48] Most importantly, this polymerization may start or stop immediately upon switching on or off visible light,[49] thus giving precise control over the targeted molecular weight and distribution of polymers. This novel technique may be well utilized for the synthesis of well-defined water-soluble polymers in the media of alcohol[50,51] or water,[48,49] and for the controlled polymerization of monomers containing acid-labile imine linkages[52] or quaternized primary amine groups.[53]

Herein, we describe a new class of PEGMA-based smart microgels, which possess entirely reversible thermally induced swellability and acid-liable dynamic properties. To the best of our awareness, such PEGMA-based smart microgels are unprecedented. To this end, an aldehyde-functionalized monomer, 3-(4-formylphenoxy)-2-hydroxypropyl methacrylate (FPHPMA, see Scheme 1), was synthesized. The well-defined copolymers of PEGMA and FPHPMA, in a variety of chain length or composition, or with different sequence, were synthesized via the visible light activating RAFT polymerization at 25 °C. The stability of aldehyde groups against air oxidation in aqueous solution at elevated solution temperature, and the effect of copolymer structure or isotopic solvent on this thermally induced phase transition was studied using ^{1}H NMR spectroscopy and dynamic light scattering (DLS). The reactivity of aldehyde groups of the thermally induced aggregates with hexamethylenediamine or adipoyl hydrazide, thermally induced swellability, and acid-liable dynamic properties of such microgels were studied in this paper.

Experimental Section

Materials. Poly(ethylene glycol) methyl ether methacrylate (PEGMA, Aldrich, M_n = 475 g mol^{-1}, M_w/M_n = 1.03) was passed through a basic alumina column to remove inhibitor and stored at −20 °C. Glycidyl methacrylate (≥98%) was purchased from Yuanji Chem. Co. Ltd., dried over 4 Å molecular sieves overnight, distilled under reduced pressure, and stored at −20 °C. 4-Hydroxybenzaldehyde (≥99.7%) was purchased from Langrui Fine Chem. Co. Ltd., tetramethylammonium bromide (>99%) was purchased from Sinopharm Chem. Reagent Co. Ltd., (2,4,6-trimethylbenzoyl)diphenylphosphine oxide (TPO, 97%) was purchased from Runtec Chem. Co., hexamethylenediamine (99.8%) was purchased from Huijing Chem. Co., adipoyl hydrazide (>99%) was from Yuancheng Tech. Develop. Co. Ltd., and *N,N*-dimethylformamide (DMF), anhydrous ethanol (99.8%), and ethyl ether were purchased from Shanghai Reagent Co.; these agents were used as received. 2-Cyanoprop-2-yl(4-fluoro)dithiobenzoate (CPFDB) was synthesized according to the literature procedures.[54] Highly pure deionized water at resistivity over 18 MΩ cm^{-1} was utilized.

Visible Light Source. A mercury vapor lamp emitting separately at 254, 302, 313, 365, 405,436, 545, and 577 nm was employed. JB400 filters purchased from Yaguang Sci. Edu. Equip. Co. were utilized to cut off UV light (λ < 400 nm) and adjust the light intensity. Thus, a visible light emitting at 405, 436, 545, and 577 nm, at mild intensity of 200 μW cm^{-2} at 420 nm, was obtained to activate the RAFT process at 25 °C.

Synthesis of 3-(4-Formylphenoxy)-2-Hydroxypropyl Methacrylate (FPHPMA) Monomer. Glycidyl methacrylate (17.48 g, 0.123 mol), 4-hydroxybenzaldehyde (15.00 g, 0.123 mol), tetramethylammonium bromide (0.947 g, 0.062 mol), and 40.0 mL of anhydrous ethanol were charged in a dried round-bottom flask being equipped with a thermometer and a reflux condenser. The solution was refluxed in nitrogen gas atmosphere under stirring at 85 °C for 10 h. The mixture was concentrated by rotary evaporation and dissolved in 40 mL of chloroform. The solution was subsequently washed using a 4.0 wt % NaOH aqueous solution, a saturated NaCl aqueous solution, and finally deionized water until it was neutralized. The solution was dried over anhydrous $MgSO_4$. After filtration, the solvent was removed by rotary evaporation. The crude product was purified by recrystallization from anhydrous ethyl ether at −18 °C and dried in vacuum at 25 °C to yield white solid product. Weight: 20.10 g; yield: 60%. ^{1}H NMR (δ, in $CDCl_3$): 9.87 ppm (1H, C_6H_4CHO), 7.00 ppm, 7.84 ppm (4H, C_6H_4CHO), 6.14 ppm, 5.60 ppm (2H, CH_2=C(CH_3)COO), 4.31−4.37 ppm (2H, COOCH_2CH(OH)CH_2O), 4.13 ppm (2H, COOCH_2CH(OH) CH_2O), 2.74 ppm (1H, CH_2CH-(O*H*)CH_2), 1.93 ppm (3H, CH_2=C(CH_3)COO).

Visible Light Activating RAFT Random Copolymerization of FPHPMA and PEGMA at 25 °C. FPHPMA (1.00 g, 3.78 mmol), PEGMA (1.796 g, 3.78 mmol), CPFDB (12.7 mg, 0.058 mmol), TPO (6.0 mg, 0.017 mmol), and 1.87 g of DMF were charged in a 25 mL round-bottom flask. This flask was capped with rubber septa and deoxygenated by purging with nitrogen gas for 30 min. The solution was irradiated with visible light under stirring at 25 °C. Samples were collected using deoxygenated syringes at predetermined intervals. The polymerization was quenched by exposure to air and adding traces of hydroquinone inhibitor. One portion of sample was diluted in $CDCl_3$ for ^{1}H NMR analysis, and another portion was diluted in DMF for GPC measurement. The monomer conversions were assessed by ^{1}H NMR analysis according to eqs 1 and 2, where $I_{9.87}$ is the integral of proton signal at δ = 9.87 ppm (C_6H_4CHO in both FPHPMA and PFPHPMA), $I_{5.62}$ is the integral of proton signal at δ = 5.62 ppm (one of CH_2=C-(CH_3)COO in FPHPMA), and $I_{5.56}$ is the integral of proton signal at δ = 5.56 ppm (one of CH_2=C(CH_3)COO in PEGMA).

$$\text{conversion}_{\text{FPHPMA}} = \frac{I_{9.87} - I_{5.62}}{I_{9.87}} \times 100\% \quad (1)$$

$$\text{conversion}_{\text{PEGMA}} = \frac{I_{9.87} - I_{5.56}}{I_{9.87}} \times 100\% \quad (2)$$

The procedure for RAFT polymerization of FPHPMA was the same as what described above, except for using a single monomer of FPHPMA.

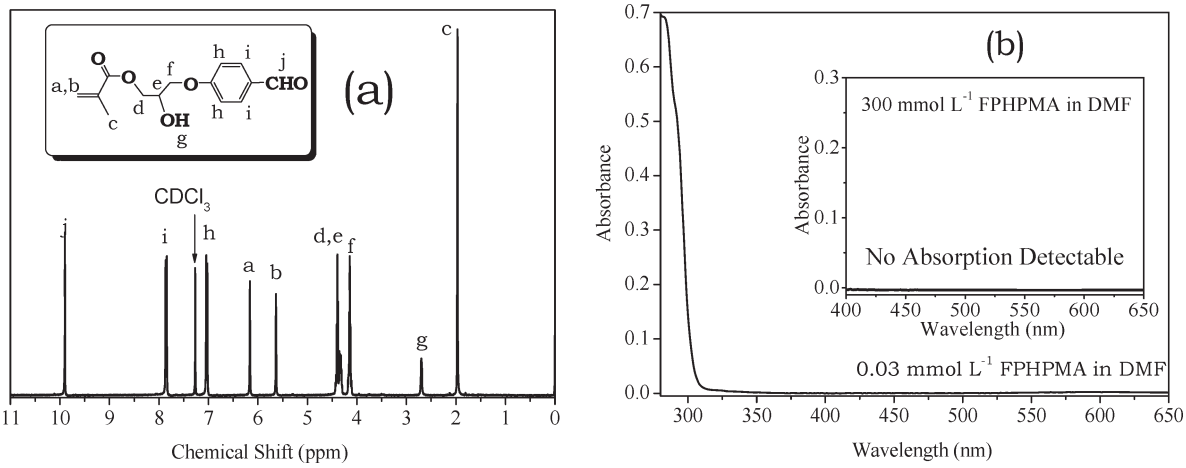

Figure 1. (a) ^{1}H NMR spectrum of 3-(4-formylphenoxy)-2-hydroxypropyl methacrylate (FPHPMA) in chloroform-*d*. (b) UV−vis spectra of 0.03 mmol L^{-1} or (inset) 300 mmol L^{-1} FPHPMA in *N,N*-dimethylformamide (DMF).

Visible Light Activating RAFT Polymerization of PEGMA Using P(FPHPMA-*ran*-PEGMA) as a Macromolecular Chain Transfer Agent (Macro-CTA) at 25 °C. P(FPHPMA$_{28}$-*ran*-PEGMA$_{18}$) (^{1}H NMR: M_n = 15.9 kg mol^{-1}; GPC: M_n = 37.6 kg mol^{-1}, M_w/M_n = 1.10; 0.856 g, 0.053 mmol), TPO (5.2 mg, 0.015 mmol), PEGMA (1.27 g, 2.65 mmol), and 1.41 g of DMF were charged in a 25 mL round-bottom flask. The flask was capped with rubber septa. The mixture was stirred to ensure full dissolving, deoxygenated by purging with nitrogen gas for 30 min. The flask was immersed in a thermostatic water bath at 25 °C, irradiated with visible light for 20 min. The solution was exposed to air and added traces of hydroquinone. 9% PEGMA monomer was polymerized according to ^{1}H NMR analysis. The copolymer was precipitated from large excess of ethyl ether and dried in a vacumm oven at 25 °C. Weight: 0.93 g; yield: 93%. ^{1}H NMR: M_n = 18.8 kg mol^{-1}; GPC: M_n = 40.2 kg mol^{-1}, M_w/M_n = 1.12.

Thermally Induced Phase Transition of Copolymers in Water. A typical procedure was as follows. 0.015 g of P(FPHPMA$_{28}$-*ran*-PEGMA$_{18}$) was dissolved in 15.0 mL of water in a 25 mL flask. The flask was immersed in ice/water bath. The solution was stirred overnight, filtered using a 0.20 μm filter. The thermally induced phase transition was studied using dynamic light scattering (DLS) analysis, including coplymers of P(FPHPMA-*ran*-PEGMA) and P(FPHPMA-*ran*-PEGMA)-*b*-PPEGMA.

Cross-Linking Reaction in Thermally Induced Aggregates. A typical procedure was as follows. 1.0 mg mL^{-1} aqueous solution of P(FPHPMA$_{28}$-*ran*-PEGMA$_{18}$) (DLS: CP = 31.4 °C, T_c = 40.5 °C; 5.1 mL, 0.009 mmol of aldehyde groups) was charged in a DLS sample vial. This vial was placed in the DLS sample cell and stabilized at 39.0 °C for 30 min. 20.1 mg g^{-1} hexamethylenediamine (28.0 mg, 0.005 mmol) or 31.1 mg g^{-1} adipoyl hydrazide (28.1 mg, 0.005 mmol) was charged in this vial. The light scattering intensity and hydrodynamic diameter were recorded at predetermined intervals.

Acid-Liable Dynamic Properties of Microgels. The solution of cross-linked copolymer microgels was cooled down to 20 °C, adjusted to perdetermined pH values using 1.0 mol L^{-1} hydrochloric acid, and stirred for 5 min prior to DLS measurements.

Analytical Techniques. *Gel permeation chromatography* (*GPC*) was performed on a PL-GPC120 setup being equipped with a column set consisting of two PL gel 5 μm MIXED-D columns (7.5 × 300 mm, effective molecular weight range of 0.2−400.0 kg mol^{-1}), using DMF as an eluent that contained 0.01 M LiBr at 80 °C, at a flow rate of 1.0 mL min^{-1}. The narrowly distributed polystyrene standards in molecular weight range of 0.5−7500.0 kg mol^{-1} (PSS, Mainz, Germany) were utilized for calibration.

^{1}*H NMR analysis* was performed on a 400 MHz Bruker AV-400 NMR spectrometer being equipped with a temperature controller. The solution temperature was precisely controlled at 25 °C.

Dynamic light scattering (*DLS*) *studies* were performed on a BI-200SM Brookhaven instrument being equipped with a 100 mW adjustable solid-state laser emitting at 532 nm, a BI-200SM goniometer, and a BI-9000 digital correlator. The laser was adjusted to 43 mW. A BI-TCD temperature controller was utilized to precisely adjust the solution temperature. The light scattering intensity and hydrodynamic diameter were recorded at an angle of 90°. The solutions were heated or cooled in steps and stabilized for 5 min before recording data.

Other Measurements. The intensity of visible light was measured using a UV-A radiometer equipped with a 420 nm sensor. UV−vis spectra were recorded using a Perkin-Elmer lamda-25 UV−vis spectrometer at 25 °C. The solution pH was measured using a PHS-3C digital pH meter.

Results and Discussion

Synthesis of 1,3-(4-Formylphenoxy)-2-Hydroxypropyl Methacrylate (FPHPMA). As shown in Scheme 1, FPHPMA was synthesized via ring-opening reaction of oxirane ring in glycidyl methacrylate (GMA) with *p*-hydroxybenzaldehyde according to the literature procedures.[55] This reaction proceeded in a dried nitrogen gas atmosphere to avoid the side reaction of oxidation or hydrolysis. On the basis of ^{1}H NMR analysis, after heating at 85 °C for 10 h, 88% GMA has been converted to FPHPMA. The crude product was recrystallized from anhydrous ethyl ether at −18 °C to give white product at a yield of 60%.

As shown in Figure 1a, the integral ratio of I_a:I_b:I_c:I_{d+e}:I_f:I_h:I_i equals 1:1:3:3:2:2:2, in good agreement with the hydrogen ratio of targeted FPHPMA. Moreover, except for the signal of chloroform-*d* impurity, no signal of other impurities is detectable. This suggests high purity of FPHPMA monomer. As shown in Figure 1b, no absorption in visible light wave range is detectable, suggesting that this FPHPMA monomer is suitable for the visible light activating ambient temperature RAFT polymerization.[49]

Visible Light Activating RAFT Polymerization of FPHPMA at 25 °C. As shown in Scheme 1 and Figure 2, at feed molar ratios of [FPHPMA]$_0$:[CPFDB]$_0$:[TPO]$_0$ = 50:1:0.3, 100:1:0.3, or 200:1:0.3, the semilogarithmic kinetic curves are linear, suggesting the first-order kinetic character of these polymerizations. This implies the constant and

steady concentration of active radicals. Moreover, increasing $[FPHPMA]_0$:$[CPFDB]_0$:$[TPO]_0$ leads to the increase of curve slope, suggesting the acceleration of polymerization. This tendency is in good agreement with what observed in RAFT polymerization of GMA monomer[56] or pyrrolidone-derived methacrylate under such mild conditions.[50] In addition, increasing $[FPHPMA]_0$:$[CPFDB]_0$:$[TPO]_0$ leads to the initialization period shortening from 22 min, 16 min, and finally to 11 min; i.e., the insertion of FPHPMA into initial CPFDB compounds was accelerated.[57,58] According to ^{1}H NMR assessment, at $[FPHPMA]_0$:$[CPFDB]_0$:$[TPO]_0$ = 200:1:0.3 in 3 h, 75% FPHPMA has been polymerized under such mild conditions.

As shown in Figure 3a, the GPC trace clearly shifts to higher molecular weight side upon increasing monomer conversions. Moreover, at monomer conversions over 30%, the GPC traces are narrow and monomodal. As shown in Figure 3b, the number-average molecular weight (M_n) linearly increases with monomer conversions. The polydispersity indices (M_w/M_n) are reasonably low at low monomer conversions, which fall down to roughly 1.20 over 30% monomer conversions. This suggests the well-controlled behavior of this polymerization.

Clearly, the molecular weights were overestimated by GPC analysis, most presumably because of the calibration errors caused by using polystyrene standards, which is less polar than PFPHPMA. Because the overestimated molecular weights by GPC analysis do not affect the tendency of molecular weight evolution with monomer conversions, this linear evolution indicates the controlled behavior of RAFT polymerization. In addition, ^{1}H NMR analysis confirmed the intact structure of PFPHPMA as synthesized under such mild conditions (Figure S1).

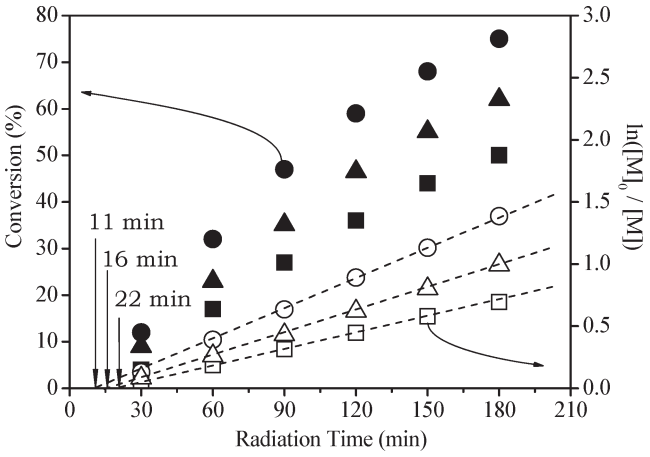

Figure 2. Kinetic curves of RAFT polymerization of 3-(4-formylphenoxy)-2-hydroxypropyl methacrylate (FPHPMA), using 2-cyanoprop-2-yl(4-fluoro)dithiobenzoate (CPFDB) chain transfer agent and (2,4,6-trimethylbenzoyl)diphenylphosphine oxide (TPO) photoinitiator in 50 wt % DMF, at feed molar ratio of (■) $[FPHPMA]_0$:$[CPFDB]_0$:$[TPO]_0$ = 50:1:0.3, (▲) $[FPHPMA]_0$:$[CPFDB]_0$:$[TPO]_0$ = 100:1:0.3, or (●) $[FPHPMA]_0$:$[CPFDB]_0$:$[TPO]_0$ = 200:1:0.3, under visible light radiation at 25 °C.

Visible Light Activating RAFT Random Copolymerization of FPHPMA and PEGMA at 25 °C. As shown in Figure 4a, at $[FPHPMA]_0$:$[PEGMA]_0$:$[CPFDB]_0$:$[TPO]_0$ = 65:65:1:0.3 in 40 wt % DMF under visible light radiation at 25 °C, the semilogarithmic kinetic curves of both monomers are linear, suggesting the well-controlled behavior of this RAFT polymerization. On the basis of the slopes of semilogarithmic kinetic curves, FPHPMA polymerizes slight more rapidly than PEGMA. However, the apparent initialization period of FPHPMA (13 min) is longer than that of PEGMA (9 min), suggesting that the insertion of PEGMA to CPFDB compounds is more rapid than FPHPMA. As shown in Figure 4b, the GPC trace clearly shifts to higher molecular weight side upon increasing monomer conversions. Moreover, as shown in Figure 4c, the M_n of copolymer linearly increases with overall monomer conversions, and M_w/M_n is lower than 1.20 at low conversion, which falls down to 1.10 at monomer conversions over 45%.

The reactivity ratio of FPHPMA and PEGMA was assessed for better understanding the structure of copolymers. Generally, the reactivity ratio was assessed according to the composition of copolymer at relatively low monomer conversion.[59,60] However, the reactivity in the initialization period or at low monomer conversion is quite different from what was observed in the propagation period at relatively high monomer conversion in living radical polymerization,[61] including RAFT polymerization. Fortunately, the concentration of active radicals is constant and steady in the

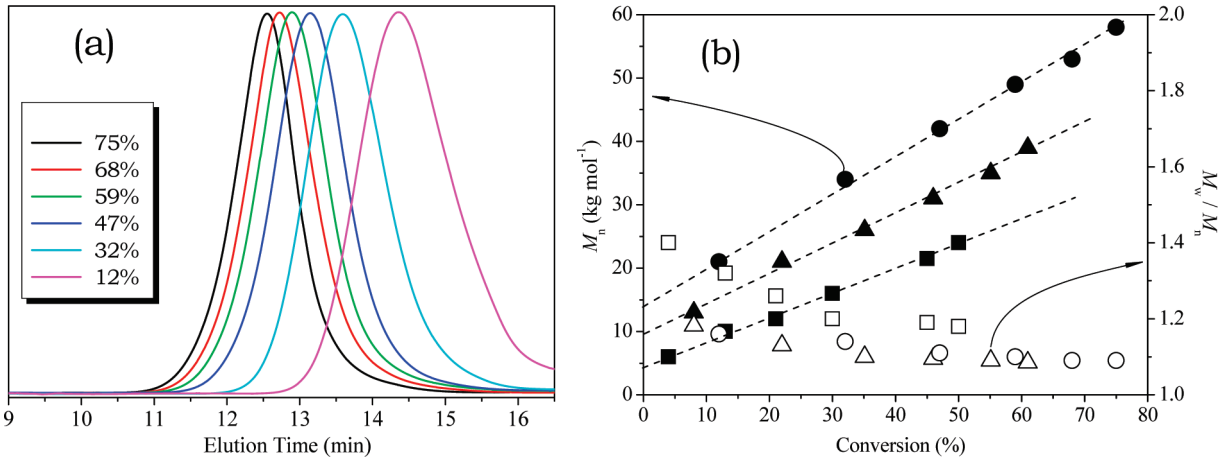

Figure 3. (a) GPC trace evolution of poly[3-(4-formylphenoxy)-2-hydroxypropyl methacrylate] (PFPHPMA) synthesized via RAFT polymerization of FPHPMA using 2-cyanoprop-2-yl(4-fluoro)dithiobenzoate (CPFDB) chain transfer agent and (2,4,6-trimethylbenzoyl)diphenylphosphine oxide (TPO) photoinitiator, at feed molar ratio of $[FPHPMA]_0$:$[CPFDB]_0$:$[TPO]_0$ = 200:1:0.3 in 50 wt % DMF, under visible light radiation at 25 °C. (b) Number-average molecular weight (M_n, solid) and polydispersity index (M_w/M_n, hollow) of PFPHPMA as a function of monomer conversions, at feed molar ratios of (■) $[FPHPMA]_0$:$[CPFDB]_0$:$[TPO]_0$ = 50:1:0.3, (▲) $[FPHPMA]_0$:$[CPFDB]_0$:$[TPO]_0$ = 100:1:0.3, or (●) $[FPHPMA]_0$:$[CPFDB]_0$:$[TPO]_0$ = 200:1:0.3.

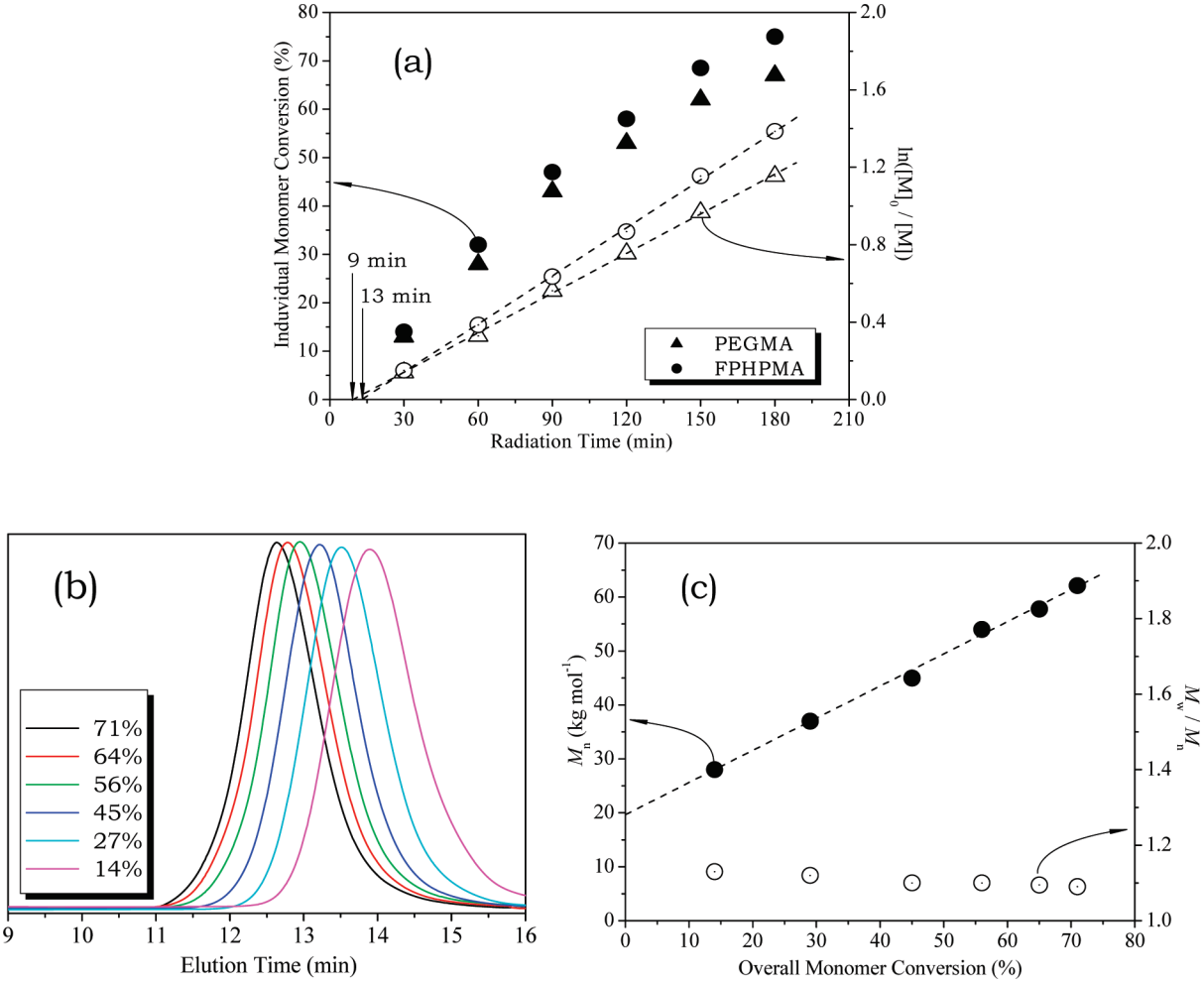

Figure 4. Kinetic curves of RAFT random copolymerization of 3-(4-formylphenoxy)-2-hydroxypropyl methacrylate (FPHPMA) and poly(ethylene glycol) methacrylate (PEGMA) using 2-cyanoprop-2-yl(4-fluoro)dithiobenzoate (CPFDB) chain transfer agent and (2,4,6-trimethylbenzoyl)-diphenylphosphine oxide (TPO) photoinitiator, at $[PEGMA]_0$:$[FPHPMA]_0$:$[CPFDB]_0$:$[TPO]_0$ = 65:65:1:0.3 in 40 wt % DMF, under visible light radiation at 25 °C. (b) GPC traces at predetermined overall monomer conversions. (c) Number-average molecular weights (M_n, solid) and polydispersity indices (M_w/M_n, hollow) of P(FPHPMA-*ran*-PEGMA) as a function of overall monomer conversions.

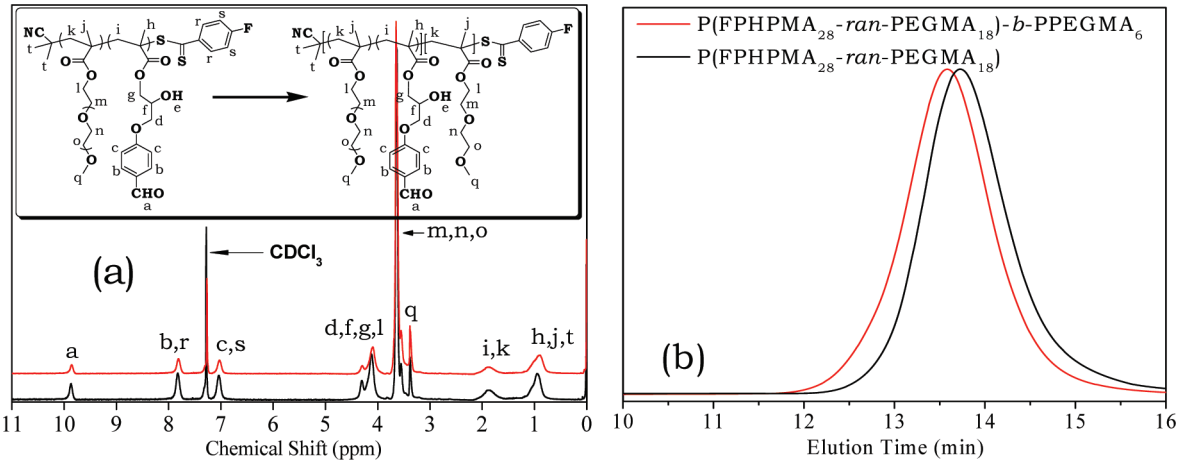

Figure 5. (a) ^{1}H NMR spectra and (b) GPC traces of P(FPHPMA$_{28}$-*ran*-PEGMA$_{18}$) (black, ^{1}H NMR: M_n = 18.6 kg mol^{-1}; GPC: M_n = 37.6 kg mol^{-1}, M_w/M_n = 1.10) and its chain-extended P(FPHPMA$_{28}$-*ran*-PEGMA$_{18}$)-*b*-PPEGMA$_6$ copolymer (red, ^{1}H NMR: M_n = 18.8 kg mol^{-1}; GPC: M_n = 40.2 kg mol^{-1}, M_w/M_n = 1.12) synthesized via RAFT polymerization of PEGMA using the above-synthesized P(FPHPMA$_{28}$-*ran*-PEGMA$_{18}$) as a macromolecular chain transfer agent and (2,4,6-trimethylbenzoyl)diphenylphosphine oxide (TPO) photoinitiator, at feed molar ratio of $[PEGMA]_0$:$[P(FPHPMA_{28}$-*ran*-$PEGMA_{18})]_0$:$[TPO]_0$ = 50:1:0.3 in 40 wt % DMF at 25 °C.

propagation period of well-controlled RAFT polymerization. Thus, is possible to precisely assess the reactivity ratio at relatively high monomer conversions. According to the extended Kelen−Tüdös method,[62] the reactivity ratio were

Table 1. Structural Parameters of P(FPHPMA-*ran*-PEGMA) (Samples 1−8) and P(FPHPMA-*ran*-PEGMA)-*b*-PPEGMA (Sample 9)[a]

sample	composition and sequence	$M_{n,^1H\ NMR}$ (kg mol^{-1})	$M_{n,GPC}$ (kg mol^{-1})	M_w/M_n	DP	molar ratio of PEGMA/FPHPMA
1	P(FPHPMA$_{28}$-*ran*-PEGMA$_{18}$)	15.9	37.6	1.10	46	0.64
2	P(FPHPMA$_{26}$-*ran*-PEGMA$_{24}$)	18.2	39.5	1.10	50	0.92
3	P(FPHPMA$_{20}$-*ran*-PEGMA$_{29}$)	19.0	40.1	1.11	49	1.45
4	P(FPHPMA$_{10}$-*ran*-PEGMA$_{38}$)	20.7	41.6	1.12	48	3.80
5	P(FPHPMA$_{59}$-*ran*-PEGMA$_{38}$)	33.6	52.9	1.14	97	0.64
6	P(FPHPMA$_{49}$-*ran*-PEGMA$_{46}$)	34.8	53.9	1.14	95	0.94
7	P(FPHPMA$_{41}$-*ran*-PEGMA$_{61}$)	39.7	54.8	1.10	102	1.49
8	P(FPHPMA$_{20}$-*ran*-PEGMA$_{78}$)	42.3	58.0	1.15	98	3.90
9	P(FPHPMA$_{28}$-*ran*-PEGMA$_{18}$)-*b*-PPEGMA$_6$	18.8	40.2	1.12	52	0.86

[a] The compositions and overall degrees of polymerization (DP) were assessed according to ^{1}H NMR analysis.

assessed to be $r_{FPHPMA} = 1.18$ and $r_{PEGMA} = 0.96$ (see Supporting Information Table S1 and Figure S2), which implies that both monomer units are statistically distributed in polymer chains.

Visible Light Activating RAFT Polymerization of PEGMA Using the Above-Synthesized P(FPHPMA-*ran*-PEGMA) as a Macro-CTA at 25 °C. As shown in Figure 5a, P(FPHPMA-*ran*-PEGMA) and its chain-extended P(FPHPMA-*ran*-PEGMA)-*b*-PPEGMA copolymer exhibit the same chemical shifts of proton signals. However, their integral ratios are different, which facilitates the composition assessment.

The proton signals of benzene rings in chain-end CPFDB residues (protons r and s, C_6H_4F) overlap with the benzene rings (protons b and c, C_6H_4CHO) of FPHPMA units at δ = 7.0−7.8 ppm, but the proton signal of aldehyde groups (proton a, C_6H_4CHO) in FPHPMA units is quite clear at δ = 9.8 ppm. In addition, the signals at δ = 3.8−4.5 ppm are attributed to the protons of both FPHPMA and PEGMA units (protons d, f, g, and l). Thus, the apparent individual degree of polymerization DP_{FPHPMA} or DP_{PEGMA} and overall DP were assessed according to eqs 3−5.

$$DP_{PFPHPMA} = \frac{2I_a}{I_{b+r} - 2I_a} \quad (3)$$

$$\frac{DP_{PEGMA}}{DP_{FPHPMA}} = \frac{I_{d+f+g+l} - 5I_a}{2I_a} \quad (4)$$

$$DP = DP_{FPHPMA} + DP_{PEGMA} \quad (5)$$

Accordingly, this random copolymer and chain-extended random−block copolymer were assessed to be P(FPHPMA$_{28}$-*ran*-PEGMA$_{18}$) and P(FPHPMA$_{28}$-*ran*-PEGMA$_{18}$)-*b*-PEGMA$_6$. As shown in Figure 5b, the GPC trace clearly shifts to higher molecular weight side after chain extension. Both GPC traces are monomodal and symmetrical at M_w/M_n = 1.10−1.12.

Thermally Induced Phase Transition of Copolymers. The well-defined copolymers were utilized to investigate their thermally induced phase transition. As shown in Table 1, the overall degrees of polymerization (DP) of samples 1−4 are ~50 but at different composition; samples 5−8 have comparable composition to those of samples 1−4 but at DP ~ 100. Sample 9 is a random−block copolymer at comparable composition and DP to the random copolymer of sample 2.

On the basis of ^{1}H NMR analysis (Figure S3), the side reaction of aldehyde oxidation in P(FPHPMA$_{28}$-*ran*-PEGMA$_{18}$) was negligible upon heating in D_2O solution in air atmosphere at 80 °C for 2 or 4 h. This is attributed to the shielding effect caused by phase separation at elevated solution temperature above the cloud point. Thus, all studies mentioned below were directly performed in an air atmosphere.

These copolymers may well dissolve in water at 20 °C. Upon heating over a critical temperature, the light scattering intensity increases sharply, suggesting the start of phase separation. This critical temperature is the so-called cloud point (CP). As shown in Figure S4, CP increases with the PEGMA fraction but decreases with copolymer concentration. This tendency was also observed in random copolymers of 2-(2-methoxyethoxy)ethyl methacrylate and PEGMA.[13]

At relatively low copolymer concentrations, further heating above another critical temperature leads to the leveling off of both light scattering intensity and hydrodynamic diameter (D_h) at low polydispersity of $\mu_2/\Gamma^2 < 0.1$. The solutions still remain transparent. This indicates the formation of compressed aggregates. This critical temerpature is denoted as T_c. However, at relatively high concentrations, heating above T_c leads to the milky solution and significant decrease of light scattering intensity, indicating that copolymer was macrophase-separated from water.

In comparison, upon heating 2.0 mg mL^{-1} P(FPHPMA$_{28}$-*ran*-PEGMA$_{18}$) over T_c (Figure S4), the light scattering intensity decreases and the solution changes to milky. However, for P(FPHPMA$_{26}$-*ran*-PEGMA$_{24}$), the milky solution is not detectable until at higher concentration of 5.0 mg mL^{-1}. This suggests that the increase of PEGMA fraction may well stabilize their aggregates.

In contrast, upon heating 5.0 mg mL^{-1} P(FPHPMA$_{28}$-*ran*-PEGMA$_{18}$)-*b*-PPEGMA$_6$ above T_c (Figure S4), the light scattering intensity levels off, and the solution is still transparent. The milky solution can only be detectable at high concentration over 20.0 mg mL^{-1}, which is significantly higher than that of P(FPHPMA$_{26}$-*ran*-PEGMA$_{24}$) at comparable composition and DP. Thus, adjusting the sequence of copolymer effectively modulates concentration dependence of this thermally induced phase transition.

On the basis of the discussion mentioned above, 1.0 mg mL^{-1} of copolymer concentration was selected to study the structural effect, including the effect of chain length, composition, or sequence on this thermally induced phase transition.

As shown in Figure 6a, for the solution of random copolymer samples at DP ~ 50, the light scattering intensity levels off upon heating above T_c, indicating the formation of compressed aggregates. The CP of copolymer increases from 31.4, 39.8, 50.0, to 75.4 °C with the unit ratio of [PEGMA]/[FPHPMA] increasing from 0.64, 0.92, 1.45, to 3.80; accordingly, T_c increases from 40.5, 51.7, to 62.9 °C and finally over 80 °C. This is attributed to the PEGMA-enhanced hydrophilicity.

As shown in Figure 6b, upon heating the solutions above CP, the copolymers start to form small irregular aggregates, as indicated by relatively higher polydispersity. Upon further heating the solutions, D_h rapidly increases, and polydispersity narrows down until the temperature reaches T_c. Thereafter, both D_h and polydispersity level off, suggesting

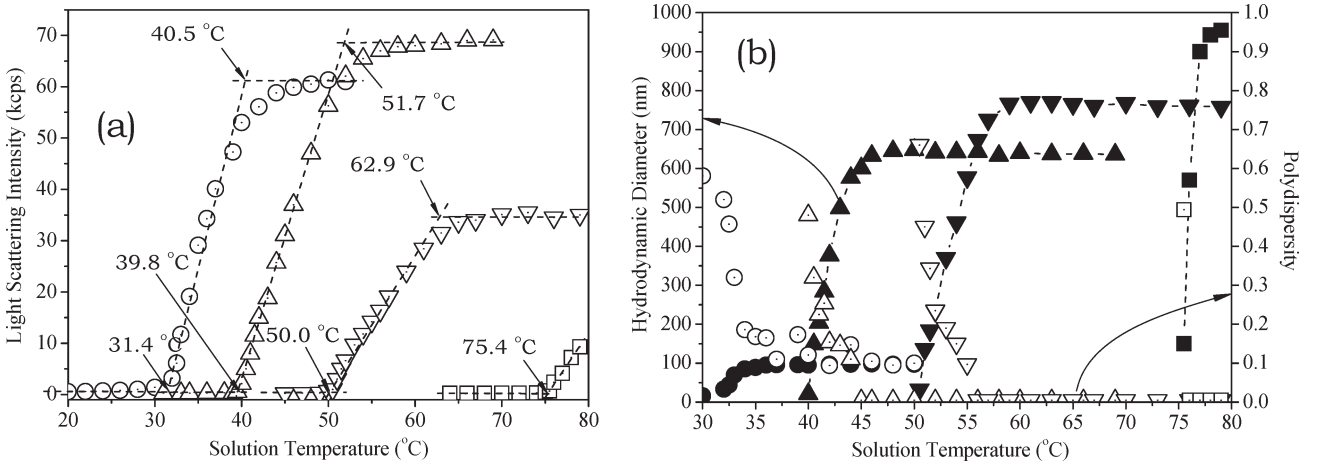

Figure 6. Evolution of (a) light scattering intensity or (b) hydrodynamic diameter (solid) and polydispersity (hollow) of 1.0 mg mL^{-1} aqueous solutions of (circle) P(FPHPMA$_{28}$-*ran*-PEGMA$_{18}$), (up triangle) P(FPHPMA$_{26}$-*ran*-PEGMA$_{24}$), (down triangle) P(FPHPMA$_{20}$-*ran*-PEGMA$_{29}$), or (square) P(FPHPMA$_{10}$-*ran*-PEGMA$_{38}$) upon heating.

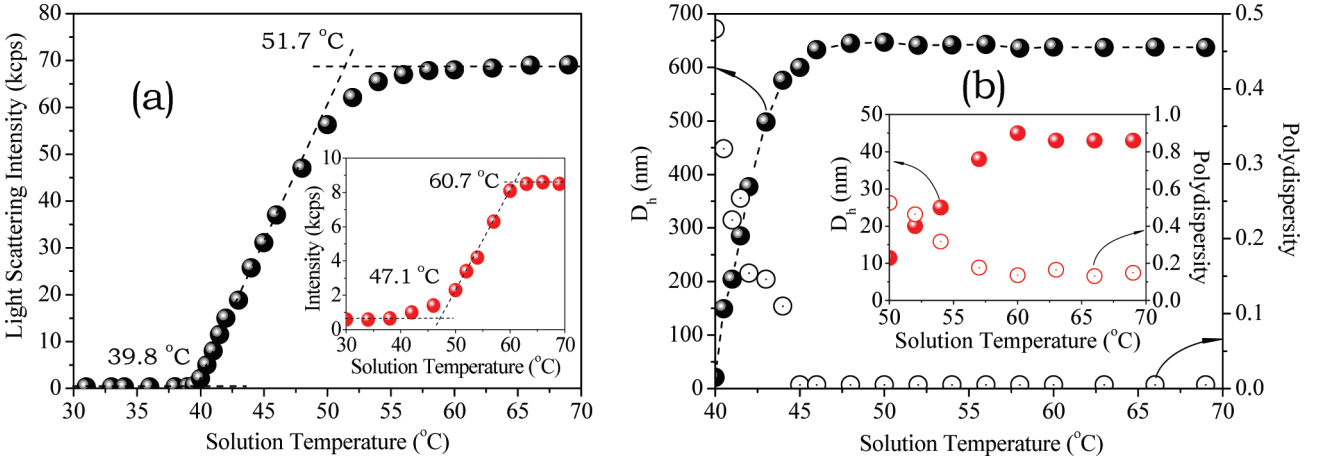

Figure 7. Evolution of (a) light scattering intensity or (b) hydrodynamic diameter (solid) and polydispersity (hollow) of 1.0 mg mL^{-1} aqueous solution of P(FPHPMA$_{26}$-*ran*-PEGMA$_{24}$) or (inset) P(FPHPMA$_{28}$-*ran*-PEGMA$_{18}$)-*b*-PPEGMA$_6$ upon heating.

the formation of well-defined compressed aggregates caused by the dehydration and collapse of PEG side chains.[17] The D_h of compressed aggregates increases from 97, 640 to 760 nm as increasing the unit ratio of [PEGMA]/[FPHPMA] from 0.64, 0.92 to 1.45.

The random copolymers at DP ~ 100 exhibit the composition dependence of phase transition similar to above-mentioned random copolymer samples at DP ~ 50, but slightly higher the CP and T_c than those at DP ~ 50 (see Figure S5). For example, CP and T_c of P(FPHPMA$_{59}$-*ran*-PEGMA$_{38}$) are separately at 32.0 and 41.7 °C, sightly higher than those of P(FPHPMA$_{28}$-*ran*-PEGMA$_{18}$) separately at 31.4 and 40.5 °C. In addition, D_h increases from 53, 540, to 695 nm as increasing the unit ratio of [PEGMA]/[FPHPMA] from 0.64, 0.94, to 1.49. This suggests that increasing chain length leads to slight increase of CP and T_c but significant decrease of particle size. This tendency most presumably attributes to the comb-shaped topology of these copolymers, which hinders the larger aggregation.

Strikingly, as shown in Figure 7, the CP of P(FPHPMA$_{26}$-*ran*-PEGMA$_{24}$) is 7.3 °C lower than P(FPHPMA$_{28}$-*ran*-PEGMA$_{18}$)-*b*-PEGMA$_6$, and its T_c is 9.0 °C lower than the latter. In addition, at the elevated solution temperature over T_c, the light scattering intensity of P(FPHPMA$_{26}$-*ran*-PEGMA$_{24}$) is 68 kcps, remarkably higher than 8.5 kcps of P(FPHPMA$_{28}$-*ran*-PEGMA$_{18}$)-*b*-PEGMA$_6$. Moreover, the D_h of P(FPHPMA$_{26}$-*ran*-PEGMA$_{24}$) aggregates is 637 nm, remarkably larger than the aggregates of P(FPHPMA$_{28}$-*ran*-PEGMA$_{18}$)-*b*-PEGMA$_6$ at D_h = 43 nm. This indicates that the random−block copolymer tends to form the regular aggregates remarkably smaller than those of random copolymer at comparable composition and DP.

As shown in Figure 8, P(FPHPMA$_{28}$-*ran*-PEGMA$_{18}$) exhibits significant hysteresis in the cooling process. Moreover, two steps of phase transition are detectable. First, cooling the solution from 44 °C down to 32 °C leads to the swelling of the aggregates from D_h = 87 to 135 nm, and decrease of light scattering intensity from 52.5 to 35.1 kcps. Upon further cooling from 32 °C down to 26 °C, both light scattering intensity and D_h dramatically decrease down to those similar to fully dissolved copolymer solution. This indicates that the swollen aggregates dissociate to small irregular aggregates up to molecularly dissolving in water. The critical dissolution temperature (27.4 °C) is 4.0 °C lower than CP (31.4 °C).

Clearly, this hysteresis is more pronounced than those observed in the random copolymers of 2-(2-methoxyethoxy)-ethyl methacrylate with PEGMA,[12] or PEGA with 2-(5,5-dimethyl-1,3-dioxan-2-yloxy)ethyl acrylate,[17] as well as the pyrrolidone-derived poly(meth)acrylates,[50,51] in which no

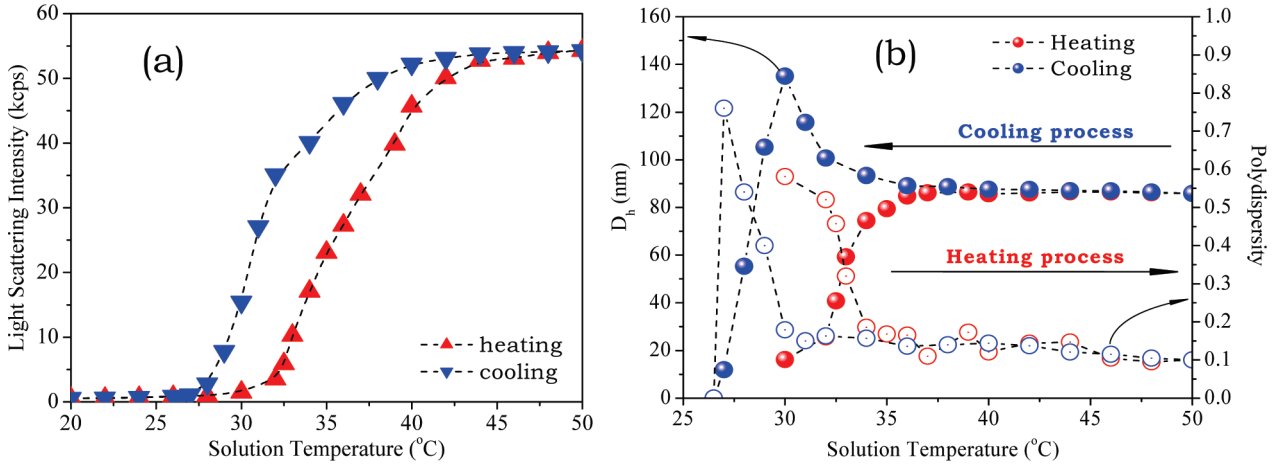

Figure 8. Evolution of (a) light scattering intensity or (b) hydrodynamic diameter (solid) and polydispersity (hollow) of 1.0 mg mL^{-1} aqueous solution of P(FPHPMA$_{28}$-*ran*-PEGMA$_{18}$) upon a cycle of heating and cooling.

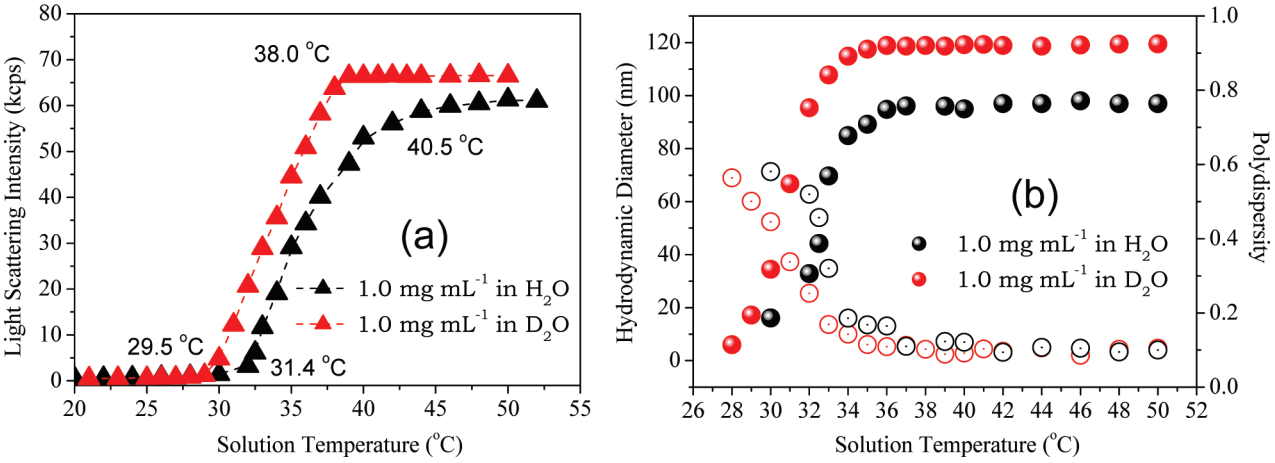

Figure 9. Evolution of (a) light scattering intensity or (b) hydrodynamic diameter (solid) and polydispersity (hollow) of 1.0 mg mL^{-1} P(FPHPMA$_{28}$-*ran*-PEGMA$_{18}$) solutions in (black) H_2O or (red) D_2O upon heating.

hydrogen donator exists for hydrogen bonding. On the contrary, this hysteresis is quite similar to what previously observed in extremely dilute solution of PNIPAM by Wu and co-workers[63,64] and in dilute solution of PNIPAM recently by Zhang and co-workers,[65] whose hysteresis attributes to the thermally induced interchain or intrachain hydrogen bonding of its amide linkages.[63−65] This indicates that the hydroxyl groups of FPHPMA units act as the hydrogen donator for hydrogen bonding. Thus, hysteresis should be attributed to the thermally induced inter- or intrachain hydrogen bonding.

As shown in Figure 9a, the CP of P(FPHPMA$_{28}$-*ran*-PEGMA$_{18}$) is 29.5 °C in heavy water (D_2O), which is 1.9 °C lower than in light water (H_2O), and the T_c of this copolymer is 38.0 °C in D_2O, which is 2.5 °C lower than in H_2O. In contrast, this lowering tendency in D_2O is contrary to what observed in PNIPAM, whose LCST is 0.4 °C higher in D_2O than in H_2O as precisely measured using dark field microscopy by Cremer and co-workers.[66]

The hydrogen bonding of PNIPAM amides with adjacent D_2O molecules is ca. 5% stronger than that with H_2O molecules;[67] thus, breaking the hydrogen bonds is more enthalpically costly in D_2O.[68] This leads to a more extended conformation[69] or higher LCST[66,69] in D_2O than in H_2O. Nevertheless, the hydrogen bonding of hydroxyl groups in P(FPHPMA$_{28}$-*ran*-PEGMA$_{18}$) chains is less strong than amide groups of PNIPAM. Moreover, the hydrophobic backbones and benzaldehyde groups of P(FPHPMA-*ran*-PEGMA) enhance the hydrophobicity. This hydrophobicity-dominated lowering tendency was observed in the pyrrolidone-derived poly(meth)acrylates,[51] in which no strong hydrogen donator exists.

As shown in Figure 9b, at elevated solution temperature over T_c, the compressed aggregates in D_2O exhibit larger D_h than in H_2O. This indicates that P(FPHPMA$_{28}$-*ran*-PEGMA$_{18}$) tends to form larger particles in D_2O than in H_2O, in the same aggregation mechanism as in H_2O.

Cross-Linking Reaction in Aggregates: Toward Microgels Possessing Entirely Reversible Thermally Induced Swellability and Acid-Liable Dynamic Properties. Hexamethylenediamine and adipoyl hydrazide were selected as cross-linkers, which may react effectively with aldehyde groups to form acid-labile dynamic imine or acylhydrazone linkages.[21−23] To ensure the swelling state of aggregates and diffusion of cross-linkers into aggregates, the solution was controlled between the CP and T_c of copolymer.

As shown in Figure 10a, upon adding hexamethylenediamine into P(FPHPMA$_{28}$-*ran*-PEGMA$_{18}$) (CP = 31.4 °C, T_c = 40.5 °C) solution at 39 °C for 6 h, the light scattering intensity gradually increases from 38 to 53.4 kcps, while D_h decreases from 85 to 80 nm. This indicates the compression of aggregates. Thereafter, both curves level off, suggesting

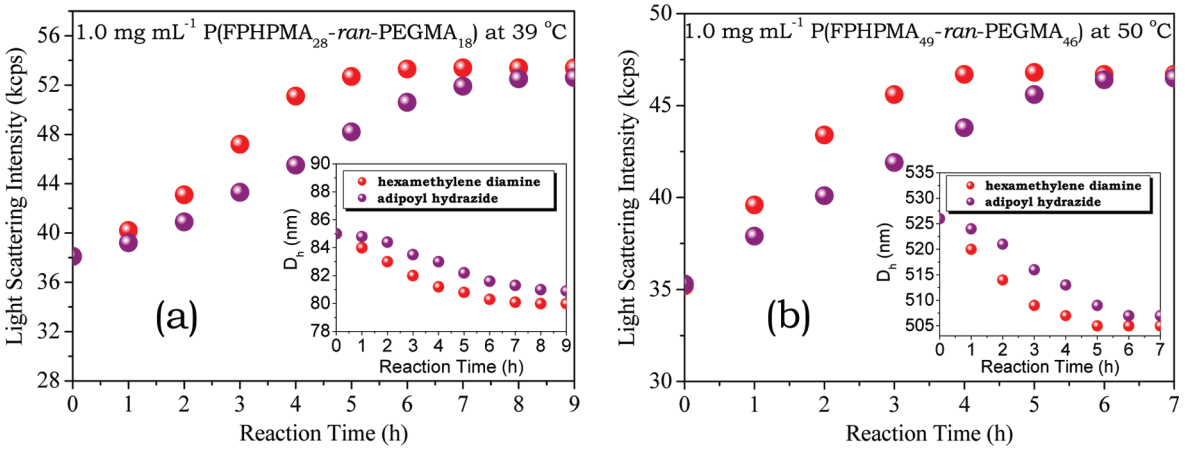

Figure 10. Evolution of light scattering intensity and hydrodynamic diameter of 1.0 mg mL^{-1} aqueous solution of (a) P(FPHPMA$_{28}$-*ran*-PEGMA$_{18}$) (CP = 31.4 °C, T_c = 40.5 °C) at 39 °C or (b) P(FPHPMA$_{49}$-*ran*-PEGMA$_{46}$) (CP = 42.8 °C, T_c = 55 °C) at 50 °C, on the addition of hexamethylenediamine (red) or adipoyl hydrazide (purple) at feed molar ratio of [aldehyde]$_0$:[hexamethylenediamine]$_0$ = 1:0.6 or [aldehyde]$_0$:[adipoyl hydrazide]$_0$ = 1:0.6.

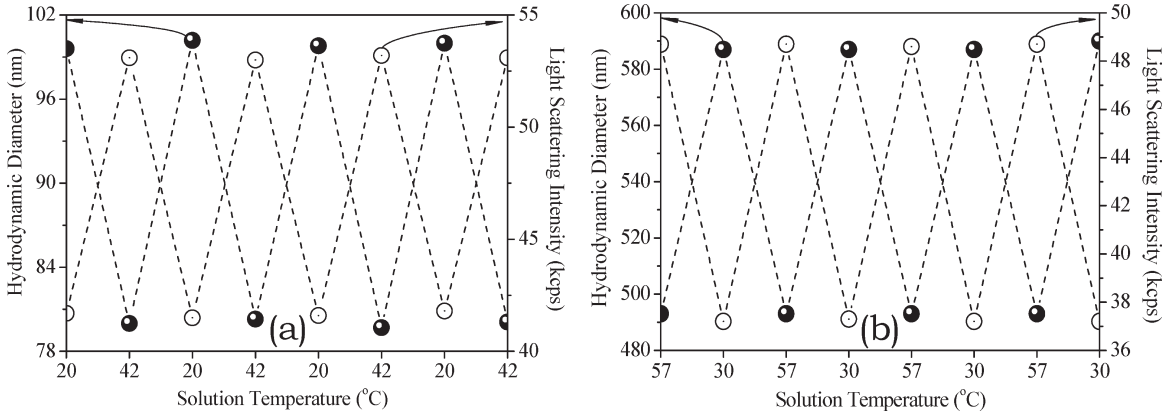

Figure 11. Evolution of light scattering intensity or hydrodynamic diameter of 1.0 mg mL^{-1} aqueous solution of (a) the microgels of P(FPHPMA$_{28}$-*ran*-PEGMA$_{18}$) (CP = 31.4 °C, T_c = 40.5 °C) cross-linked by adipoyl hydrazide upon heating to 42 °C and cooling to 20 °C repeatedly or (b) the microgels of P(FPHPMA$_{49}$-*ran*-PEGMA$_{46}$) (CP = 42.8 °C, T_c = 55 °C) cross-linked by hexamethylenediamine upon heating to 57 °C and cooling to 30 °C repeatedly.

that this reaction has reached equilibrium of reaction. In the whole process, the polydispersity keeps essentially constant at $\mu_2/\Gamma^2 \sim 0.10$, indicating that no coacervation occurs in this cross-linking process. In comparison, upon adding adipoyl hydrazide, the shrinking process carried out in ca. 8 h, 2 h longer than the former. This suggests that adipoyl hydrazide is less reactive than hexamethylenediamine. Moreover, after reaching equilibrium, the light scattering intensity increases to 52.5 kcps and D_h descreases to 81 nm, which is lower than 53.4 kcps and larger than 80 nm of the former. This indicates the formation of larger and looser aggregates as compared with the former. This attributes to the more hydrophobicity of imine linkages than acylhydrazone linkages.

As shown in Figure 10b, a similar shrinking process was also observed in P(FPHPMA$_{49}$-*ran*-PEGMA$_{46}$) (CP = 42.8 °C, T_c = 55 °C) solution at 50 °C, in which the reaction was carried out in relatively large aggregates.

Moreover, cooling the solution of cross-linked aggregates of P(FPHPMA$_{28}$-*ran*-PEGMA$_{18}$) down to T_c, the light scattering intensity decreases and D_h increases (Figure S6), suggesting the swelling of aggregates. However, upon further cooling the solution well below CP, both light scattering intensity and D_h level off separately at 40 kcps and 97 nm, remarkably higher than those observed in the solution of its corresponding non-cross-linked copolymer. This demonstrates the formation of stabilized microgels.

As shown in Figure 11a, upon heating or cooling the solution repeatedly, the microgels of P(FPHPMA$_{28}$-*ran*-PEGMA$_{18}$) cross-linked by hyexamethylenediamine repeatably shrink to D_h = 80 nm at 42 °C or swell to D_h = 100 nm at 20 °C. As shown in Figure 11b, the reversible thermally induced swellability was also observed in the microgels of P(FPHPMA$_{49}$-*ran*-PEGMA$_{46}$) cross-linked by adipoyl hydrazide. This indicates that their thermally induced swellability was entirely reversible, cross-linked by either hyexamethylenediamine or adipoyl hydrazide.

As shown in Figure 12, for the solution of microgels cross-linked by hyexamethylenediamine, both light scattering intensity and D_h are constant in alkali solution at 20 °C. However, upon acidifying solution from pH 7.43 to 5.82, the microgels have been swollen from D_h = 98 nm to D_h = 149 nm. This is attributed to the hydrolysis of imine linkages, which leads to the decrease of cross-linking density.

Interestingly, upon heating this solution up to 39 °C and adjusting the solution back to pH 9.0, the aggregates exhibit the same swellability as that observed in the initial microgels. This indicates the entirely reversible acid-liable swellability. Therefore, the acid-liable dynamic behavior may well adjust the swellability of these microgels.

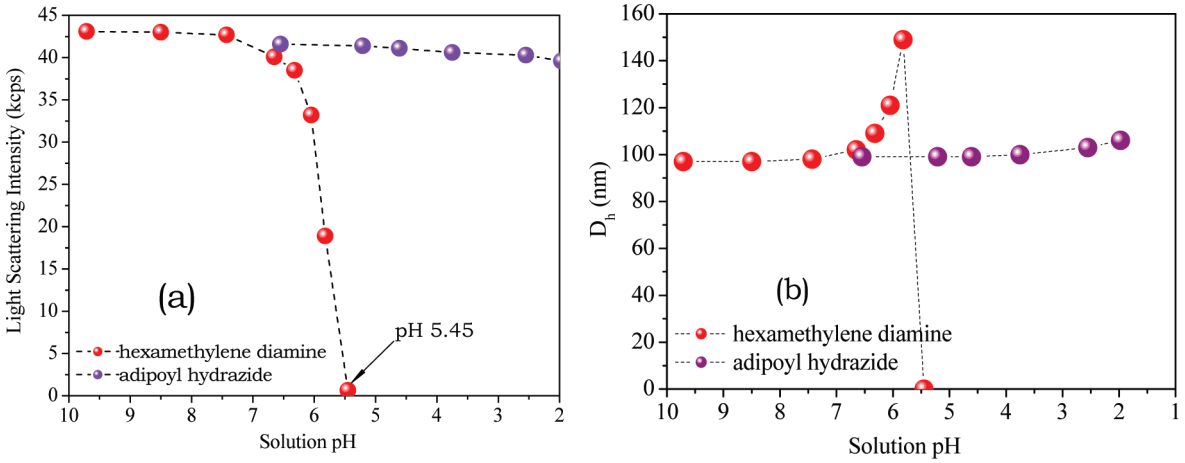

Figure 12. Evolution of (a) light scattering intensity and (b) hydrodynamic diameter of 1.0 mg mL^{-1} aqueous solution of microgels of P(FPHPMA$_{28}$-*ran*-PEGMA$_{18}$) upon adjusting the solution pH at 20 °C. Red: cross-linked by hexamethylenediamine; purple: cross-linked by adipoyl hydrazide.

Further lowering solution pH down to 5.45, the microgels are completely dissociated, leading to dramatic decrease of both light scattering intensity and D_h to what observed in the fully dissolved solution. Clearly, in such acidic solution, the imine linkages have been completely hydrolyzed.[70]

In contrast, as shown in Figure 12, the microgels cross-linked by adipoyl hydrazide were stable in acidic solution down to pH 2.0 because of the excellent stability of acylhydrazone linkages in acidic solution.[71] Further acidifying the solution down to pH 1.0 leads to the hydrolysis of both acylhydrazone and ester linkages.

Conclusion

This paper described a new class of the PEGMA-based smart microgels, which have entirely reversible thermally induced swellability and acid-liable dynamic properties. To this end, an aldehyde-functionalized FPHPMA monomer was synthesized. RAFT polymerization of FPHPMA, RAFT random copolymerization of FPHPMA and PEGMA, and chain extension RAFT polymerization of PEGMA using a P(FPHPMA-*ran*-PEGMA) macro-CTA proceeded under visible light radiation at 25 °C. The results indicated the well-controlled polymerization of FPHPMA, comparable reactivity of FPHPMA and PEGMA, and living character of these polymerizations under such mild conditions. Thus, a range of well-defined copolymers of FPHPMA and PEGMA with different chain length, composition, or sequence were synthesized.

These copolymers well dissolved in water at low temperature and exhibited a cloud point (CP) and a critical temperature for formation of compressed aggregates (T_c) upon heating. The aldehyde groups of copolymers were stable against air oxidation in water at 80 °C. Increasing copolymer concentration led to the decrease of CP and T_c. The phase transition of random copolymers were slightly influenced by chain length but significantly affected by composition; increasing the PEGMA fraction led to the increase of CP and T_c and larger aggregates. Moreover, the sequence of copolymers is an important factor to control over this thermally induced phase transition. Contrary to previously reported PEGMA-based copolymers, these copolymers exhibited significant hysteresis in cooling process, which is similar to what observed in PNIPAM. However, their isotopic solvent effect was contrary to what observed in PNIPAM.

In these thermally induced aggregates, the aldehyde groups may react well with hexamethylenediamine or adipoyl hydrazide, leading to the formation of stabilized microgels. These microgels exhibited entirely reversible thermally induced swellability. The acid-liable dynamic behavior of imine linkages could tune the cross-linking density of microgels, thus adjusting their thermally induced swellability. The detailed studies on dynamic cross-linking and exploiting for carriers of amino acids are currently in progress, and we are going to report in a following paper.

Acknowledgment. We thank the National Natural Science Foundation of China (20874081, 21074104, 20674064), the Research Fund for Doctoral Program of Higher Education of China (200805300004), and the Scientific Research Fund of Hunan Provincial Education Department (10A116) for financial support of this research.

Supporting Information Available: Kelen−Tüdös parameters and plot for RAFT random copolymerization of FPHPMA and PEGMA; ^{1}H NMR spectrum of PFPHPMA homopolymer; ^{1}H NMR spectra of D_2O solution of P(FPHPMA-*ran*-PEGMA) before or after heating in air at 80 °C; the concentration dependence of light scattering intensity of copolymer solutions upon heating, light scattering intensity and hydrodynamic diameter of the solutions of random copolymer at DP ~ 100 upon heating, and light scattering intensity and hydrodynamic diameter of cross-linked microgels upon cooling. This material is available free of charge via the Internet at http://pubs.acs.org.

References and Notes

(1) Duncan, R. *Nature Rev. Drug Discovery* **2003**, *2*, 347–360.
(2) Pasut, G.; Veronese, F. M. *Adv. Polym. Sci.* **2006**, *192*, 95–134.
(3) Zhao, B.; Li, D.; Hua, F.; Green, D. R. *Macromolecules* **2005**, *38*, 9509–9517.
(4) Magnusson, J. P.; Khan, A.; Pasparakis, G.; Saeed, A. O.; Wang, W.; Alexander, C. *J. Am. Chem. Soc.* **2008**, *130*, 10852–10853.
(5) Zarafshani, Z.; Obata, T.; Lutz, J.-F. *Biomacromolecules* **2010**, *11*, 2130–2135.
(6) Han, S.; Hagiwara, M.; Ishizone, T. *Macromolecules* **2003**, *26*, 8312–8319.
(7) Ali, M. M.; Stöver, H. D. H. *Macromolecules* **2004**, *37*, 5219–5227.
(8) Sugihara, S.; Kanaoka, S.; Aoshima, S. *Macromolecules* **2005**, *38*, 1919–1927.
(9) Boyer, C.; Whittaker, M. R.; Luzon, M.; Davis, T. P. *Macromolecules* **2009**, *42*, 6917–6926.
(10) Wang, W.; Liang, H.; Ghanami, R. C. A.; Hamilton, L.; Fraylich, M.; Shakesheff, K. M.; Saunders, B.; Alexander, C. *Adv. Mater.* **2009**, *21*, 1809–1813.
(11) Dong, H.; Matyjaszewski, K. *Macromolecules* **2010**, *43*, 4623–4628.
(12) Lutz, J.-F.; Akdemir, Ö.; Hoth, A. *J. Am. Chem. Soc.* **2006**, *128*, 13046–13047.

(13) Lutz, J.-F.; Hoth, A. *Macromolecules* **2006**, *39*, 893–896.
(14) Lutz, J.-F.; Weichenhan, K.; Akdemir, Ö.; Hoth, A. *Macromolecules* **2007**, *40*, 2503–2508.
(15) Skrabania, K.; Kristen, J.; Laschewsky, A.; Akdemir, Ö.; Hoth, A.; Lutz, J.-F. *Langmuir* **2007**, *23*, 84–93.
(16) Morinaga, H.; Morikawa, H.; Wang, Y.; Sudo, A.; Endo, T. *Macromolecules* **2009**, *42*, 2229–2235.
(17) Qiao, Z.; Du, F.; Zhang, R.; Liang, D.; Li, Z. *Macromolecules* **2010**, *43*, 6485–6494.
(18) Zhang, J.; Jiang, X.; Zhang, Y.; Li, Y.; Liu, S. *Macromolecules* **2007**, *40*, 9125–9132.
(19) Liu, H.; Jiang, X.; Fan, J.; Wang, G.; Liu, S. *Macromolecules* **2007**, *40*, 9074–9083.
(20) Hawker, C. J.; Wooley, K. L. *Science* **2005**, *309*, 1200–1205.
(21) Slomkowski, S. *Prog. Polym. Sci.* **1998**, *23*, 815–874.
(22) Slomkowski, S.; Basinska, T.; Miksa, B. *Polym. Adv. Technol.* **2002**, *13*, 906–918.
(23) Salo, H.; Virta, P.; Hakala, H.; Prakash, T. P.; Kawasaki, A. M.; Manoharan, M.; Lonnberg, H. *Bioconjugate Chem.* **1999**, *10*, 815–823.
(24) Iijima, M.; Kato, M.; Kataoka, K. *Macromolecules* **1998**, *31*, 1473–1479.
(25) Nagasaki, Y.; Okada, T.; Scholz, C.; Akiyama, Y.; Harada, A.; Nagasaki, Y.; Kataoka, K. *Macromolecules* **2000**, *33*, 5841–5845.
(26) Wakebayashi, D.; Nishiyama, N.; Yamasaki, Y.; Itaka, K.; Kanayama, N.; Harada, A.; Nagasaki, Y.; Kataoka, K. *J. Controlled Release* **2004**, *95*, 653–664.
(27) Ishii, T.; Otsuka, H.; Kataoka, K.; Nagasaki, Y. *Langmuir* **2004**, *20*, 561–564.
(28) Chiefari, J.; Chong, Y. K. B.; Ercole, F.; Krstina, J.; Jeffery, J.; Le, T. P. T.; Mayadunne, R. T. A.; Meijs, G. F.; Moad, C. L.; Moad, G.; Rizzardo, E.; Thang, S. H. *Macromolecules* **1998**, *31*, 5559–5562.
(29) Schilli, C. M.; Zhang, M.; Rizzardo, E.; Thang, S. H.; Chong, Y. K.; Edwards, K.; Karlsson, G.; Müller, A. H. E. *Macromolecules* **2004**, *37*, 7861–7866.
(30) Li, Y.; Lokitz, B. S.; Armes, S. P.; McCormick, C. L. *Macromolecules* **2006**, *39*, 2726–2728.
(31) Zhang, J.; Jiang, X.; Zhang, Y.; Li, Y.; Liu, S. *Macromolecules* **2007**, *40*, 9125–9132.
(32) De, P.; Li, M.; Gondi, S. R.; Sumerlin, B. S. *J. Am. Chem. Soc.* **2008**, *130*, 11288–11289.
(33) Boyer, C.; Bulmus, V.; Davis, T. P.; Ladmiral, V.; Liu, J.; Perrier, S. *Chem. Rev.* **2009**, *109*, 5402–5436.
(34) Shi, M.; Li, A.-L.; Liang, H.; Lu, J. *Macromolecules* **2007**, *40*, 1891–1896.
(35) Hwang, J.; Li, R. C.; Maynard, H. D. *J. Controlled Release* **2007**, *122*, 279–286.
(36) Sun, G.; Cheng, C.; Wooley, K. L. *Macromolecules* **2007**, *40*, 793–795.
(37) Sokolsky-Papkov, M.; Domb, A. J.; Golenser, J. *Biomacromolecules* **2006**, *7*, 1529–1535.
(38) Hwang, J.; Li, R.; Maynard, H. D. *J. Controlled Release* **2007**, *122*, 279–286.
(39) Rossi, N. A. A.; Zou, Y.; Scott, M. D.; Kizhakkedathu, J. N. *Macromolecules* **2008**, *41*, 5272–5282.
(40) Sun, G.; Cheng, C.; Wooley, K. L. *Macromolecules* **2007**, *40*, 793–795.
(41) Sun, G.; Fang, H.; Cheng, C.; Lu, P.; Zhang, K.; Walker, A. V.; Taylor, J.-S. A.; Wooley, K. L. *ACS Nano* **2009**, *3*, 673–681.
(42) Shi, M.; Li, A.; Liang, H.; Lu, J. *Macromolecules* **2007**, *40*, 1891–1896.
(43) Xiao, N.; Li, A.; Liang, H.; Lu, J. *Macromolecules* **2008**, *41*, 2374–2380.
(44) Lu, L.; Yang, N.; Cai, Y. *Chem. Commun.* **2005**, 5287–5288.
(45) Lu, L.; Zhang, H.; Yang, N.; Cai, Y. *Macromolecules* **2006**, *39*, 3770–3776.
(46) Jiang, W.; Lu, L.; Cai, Y. *Macromol. Rapid Commun.* **2007**, *28*, 725–728.
(47) Li, Y.; Tang, Y.; Yang, K.; Chen, X.; Lu, L.; Cai, Y. *Macromolecules* **2008**, *41*, 4597–4606.
(48) Shi, Y.; Gao, H.; Lu, L.; Cai, Y. *Chem. Commun.* **2009**, 1368–1370.
(49) Shi, Y.; Liu, G.; Gao, H.; Lu, L.; Cai, Y. *Macromolecules* **2009**, *42*, 3917–3926.
(50) Deng, J.; Shi, Y.; Jiang, W.; Peng, Y.; Lu, L.; Cai, Y. *Macromolecules* **2008**, *41*, 3007–3014.
(51) Sun, J.; Peng, Y.; Chen, Y.; Liu, Y.; Deng, J.; Lu, L.; Cai, Y. *Macromolecules* **2010**, *43*, 4041–4049.
(52) Luo, Q.; Zheng, H.; Peng, Y.; Gao, H.; Lu, L.; Cai, Y. *J. Polym. Sci., Polym. Chem.* **2009**, *47*, 6668–6681.
(53) Gao, H.; Liu, G.; Chen, X.; Hao, Z.; Tong, J.; Lu, L.; Cai, Y.; Long, F.; Zhu, M. *Macromolecules* **2010**, *43*, 6156–6165.
(54) Benaglia, M.; Rizzardo, E.; Alberti, A.; Guerra, M. *Macromolecules* **2005**, *38*, 3129–3140.
(55) Olszewski-Ortar, A.; Gros, P.; Fort, Y. *Tetrahedron Lett.* **1997**, *38*, 8699–8702.
(56) Yin, H.; Zheng, H.; Lu, L.; Liu, P.; Cai, Y. *J. Polym. Sci., Polym. Chem.* **2007**, *22*, 5091–5102.
(57) McLeary, J. B.; McKenzie, J. M.; Tonge, M. P.; Sanderson, R. D.; Klumperman, B. *Chem. Commun.* **2004**, 1950–1951.
(58) McLeary, J. B.; Calitz, F. M.; McKenzie, J. M.; Tonge, M. P.; Sanderson, R. D.; Klumperman, B. *Macromolecules* **2004**, *37*, 2383–2394.
(59) Mayo, F. R.; Lewis, F. M. *J. Am. Chem. Soc.* **1944**, *66*, 1594–1601.
(60) Kennedy, J. P.; Kelen, T.; Tüdös, F. *J. Polym. Sci., Polym. Chem.* **1975**, *13*, 2277–2289.
(61) Madruga, E. L. *Prog. Polym. Sci.* **2002**, *27*, 1879–1924.
(62) Kelen, T.; Tüdös, F.; Turcsányi, B. *J. Polym. Sci., Polym. Chem.* **1977**, *15*, 3047–3074.
(63) Wu, C.; Wang, X. *Phys. Rev. Lett.* **1998**, *80*, 4092–4094.
(64) Wang, X.; Qiu, X.; Wu, C. *Macromolecules* **1998**, *31*, 2972–2976.
(65) Tang, Y.; Ding, Y.; Zhang, G. *J. Phys. Chem. B* **2008**, *112*, 8447–8451.
(66) Mao, H.; Li, C.; Zhang, Y.; Furyk, S.; Cremer, P. S.; Bergbreiter, D. E. *Macromolecules* **2004**, *37*, 1031–1036.
(67) Nemethy, G.; Scheraga, H. A. *J. Chem. Phys.* **1964**, *41*, 680–689.
(68) Sun, B.; Lin, Y.; Wu, P.; Siesler, H. W. *Macromolecules* **2008**, *41*, 1512–1520.
(69) Wang, X.; Wu, C. *Macromolecules* **1999**, *32*, 4299–4301.
(70) Minkenberg, C. B.; Florusse, L.; Eelkema, R.; Koper, G. J. M.; van Esch, J. H. *J. Am. Chem. Soc.* **2009**, *131*, 11274–11275.
(71) Gasparini, G.; Bettin, F.; Scrimin, P.; Prins, L. J. *Angew. Chem., Int. Ed.* **2009**, *48*, 4546–4550.